



*Supplement of*

## **Biochemical characteristics of the sea surface microlayer in the central Baltic Sea and potential signatures of cyanobacterial blooms**

**Josefine Karnatz et al.**

*Correspondence to:* Josefine Karnatz ([jkarnatz@geomar.de](mailto:jkarnatz@geomar.de))

The copyright of individual parts of the supplement might differ from the article licence.

# Supplements

## 1. Methods

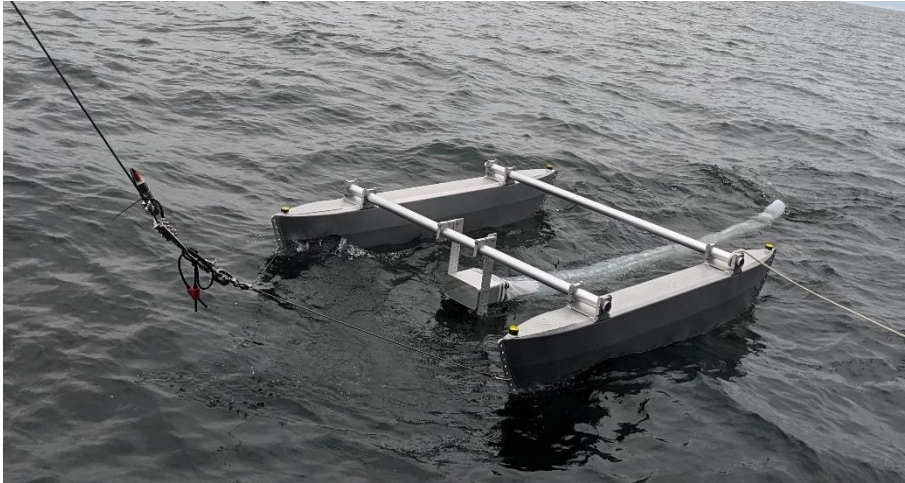


**Figure S 1:** Neuston catamaran equipped with a 20  $\mu\text{m}$  phytoplankton net was towed parallel to the research vessel.

5

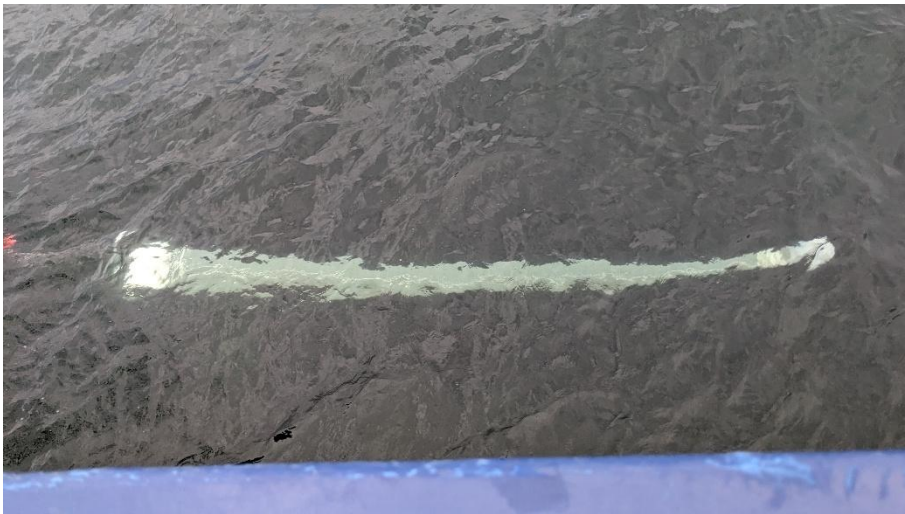
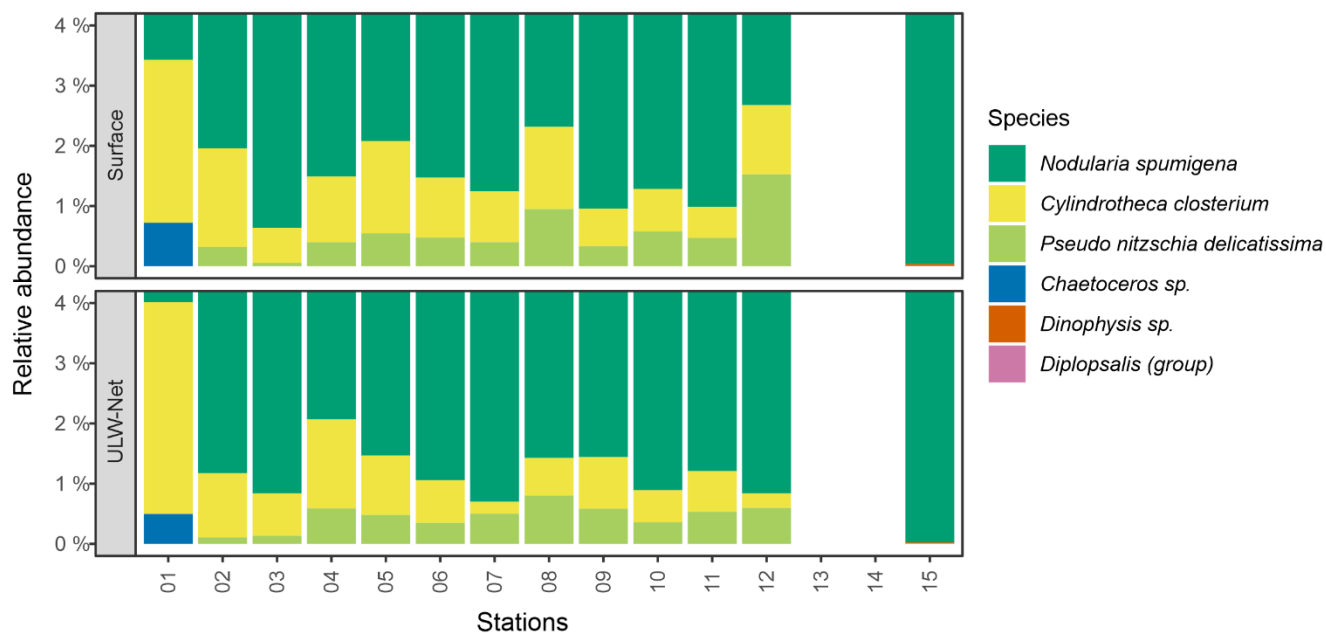


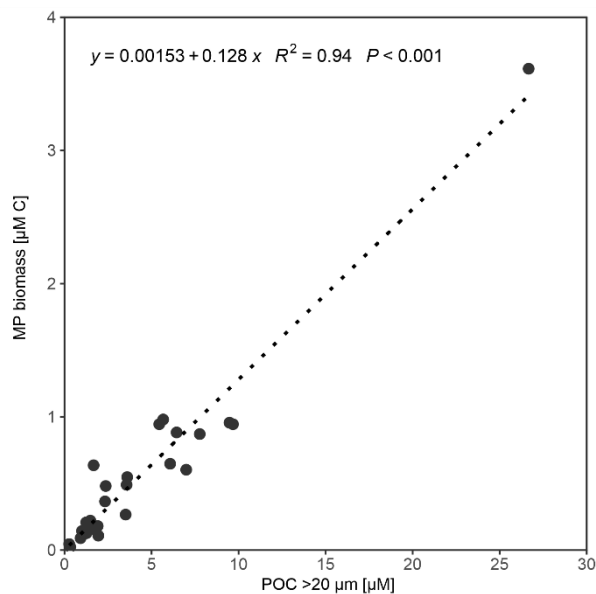
**Figure S 2:** ULW net with a 20  $\mu\text{m}$  mesh size was towed parallel to the research vessel at approx. 1 m depth.

10

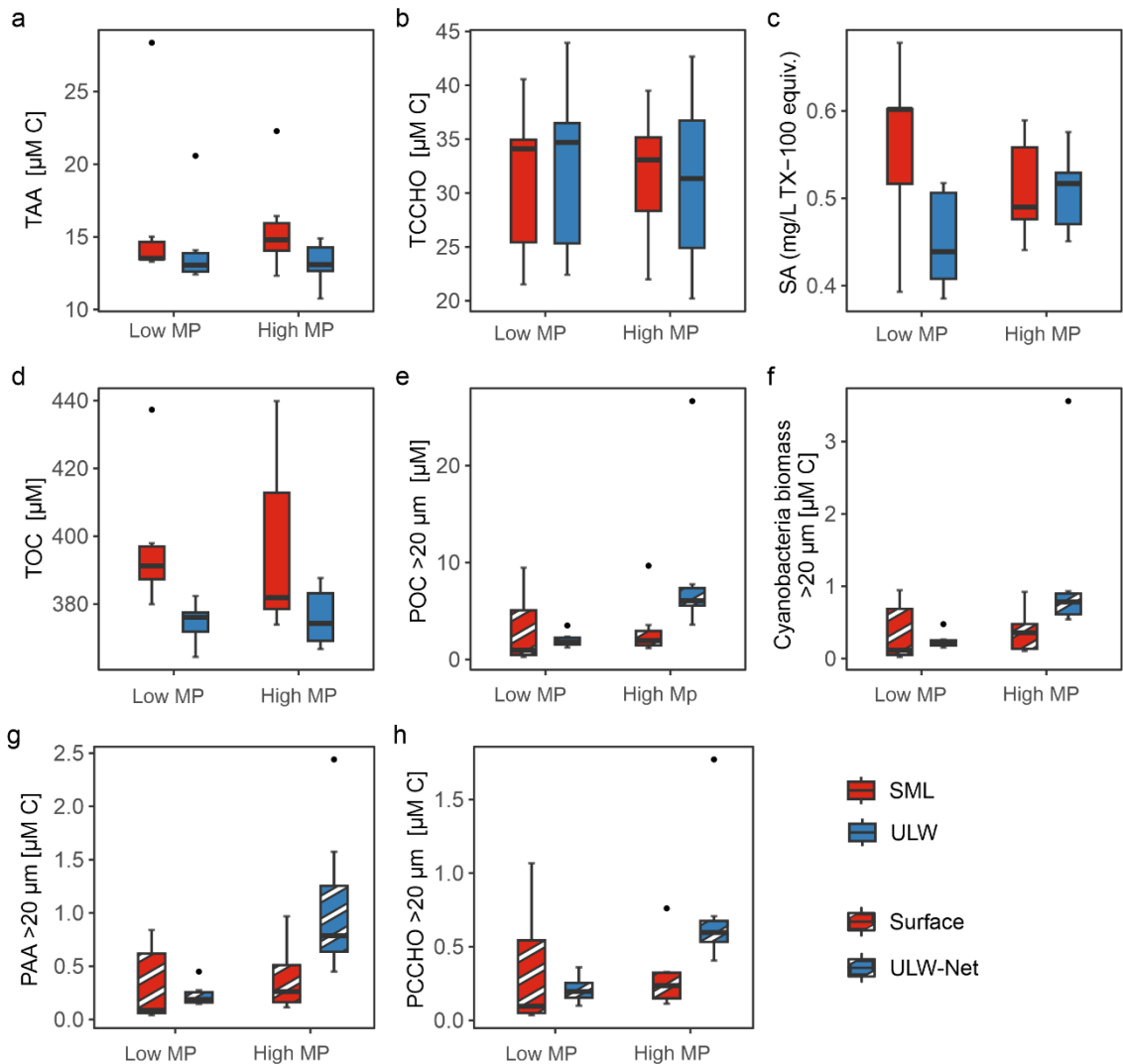
## 2. Results



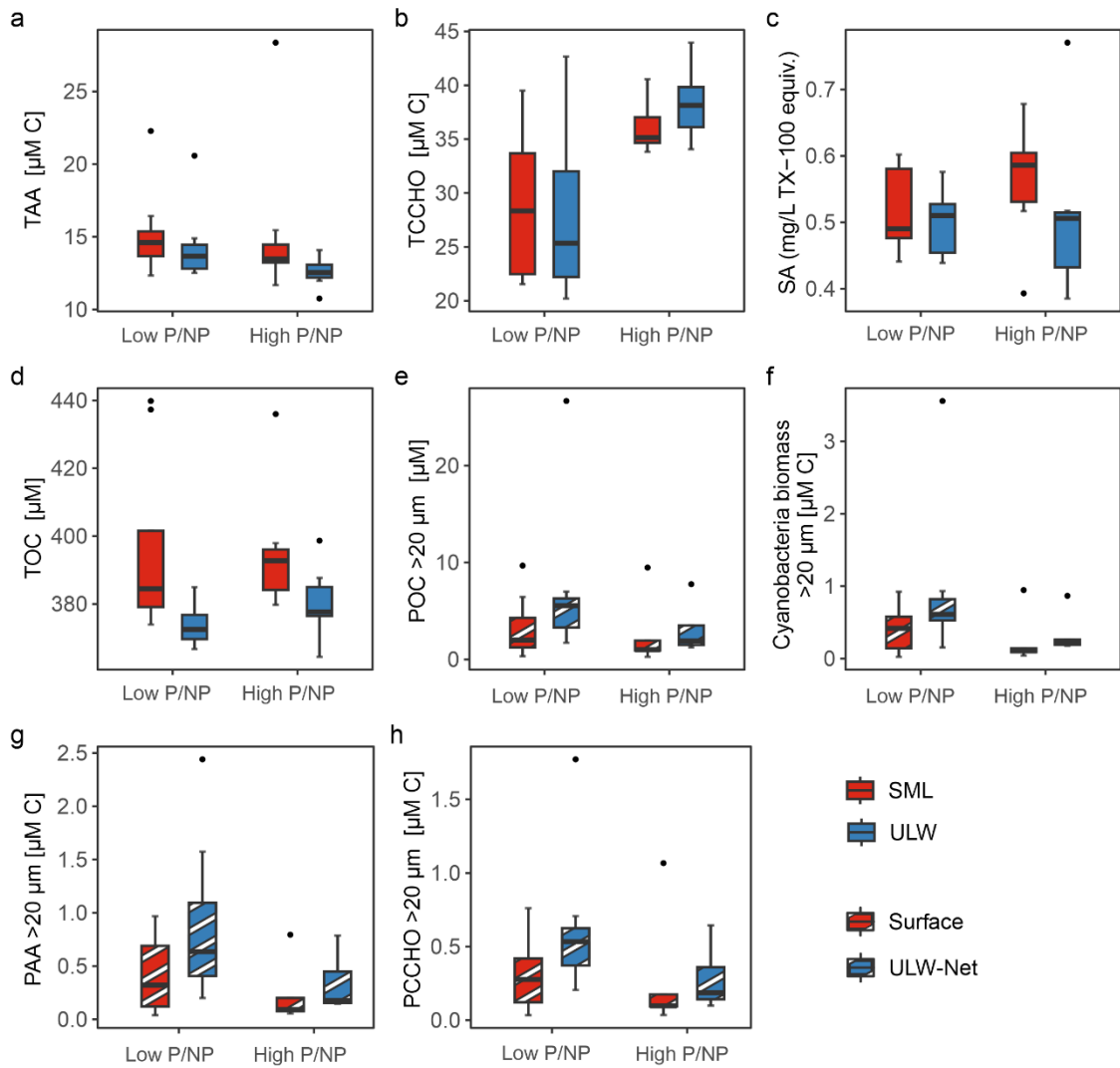
15 **Figure S 3:** Stacked bar plots of the relative abundance of the six major microphytoplankton taxa out of the eight identified taxa in (top) Surface net samples and (bottom) ULW-Net samples (both >20  $\mu\text{m}$  fraction). Relative abundances are shown below 4%. *Dinophysis sp.* and *Diplopsalis (group)* were only present at station 15 with less than 0.1%.



20 **Figure S 4:** Linear regression between POC >20  $\mu\text{m}$  and microphytoplankton (MP, >20  $\mu\text{m}$ ) biomass. The regression equation is displayed in the plot, along with the corresponding coefficient ( $R^2$ ) and  $p$ -value.



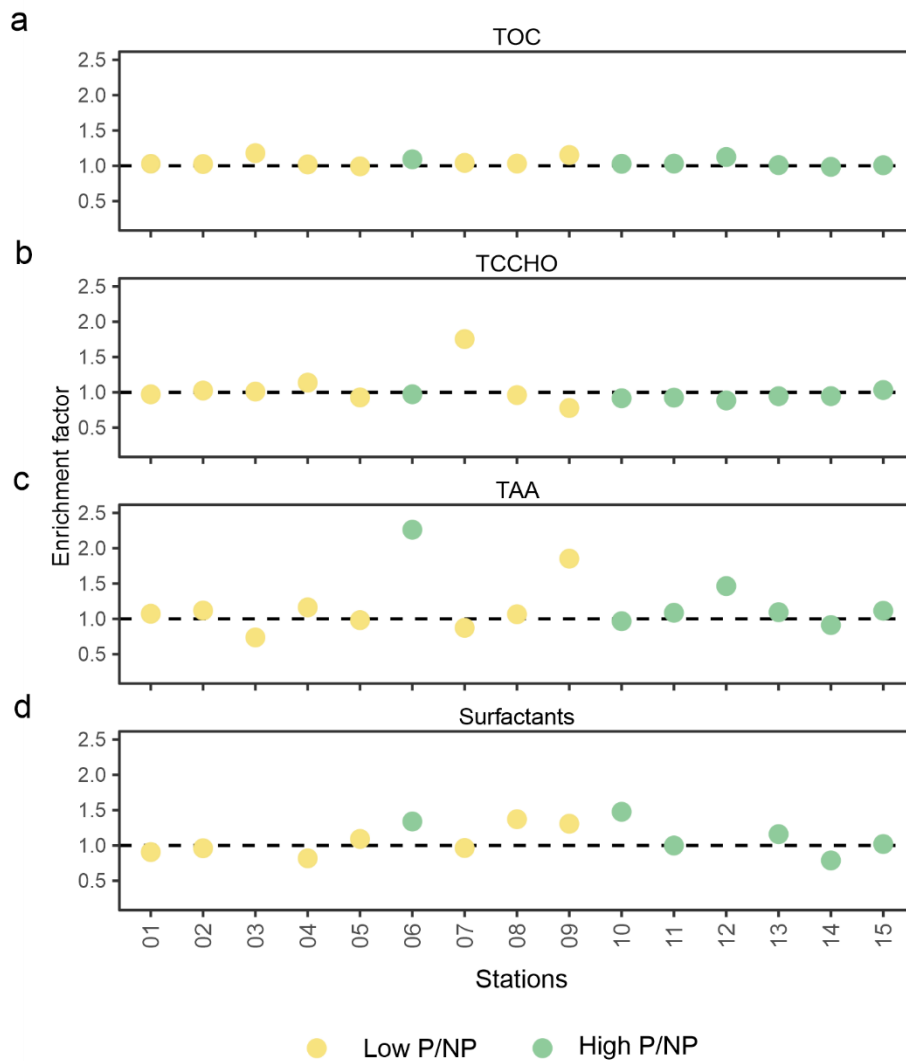
25 **Figure S 5:** Concentration differences during low microphytoplankton (Low MP) and high microphytoplankton (High MP) abundance conditions for (a) total amino acids (TAA), (b) total combined carbohydrates (TCCHO), (c) surfactants (SA), (d) total organic carbon (TOC), (e) particulate organic carbon (POC) >20  $\mu\text{m}$ , (f) cyanobacteria biomass >20  $\mu\text{m}$ , (g) particulate amino acids (PAA) >20  $\mu\text{m}$  and (h) particulate combined carbohydrates (PCCHO) >20  $\mu\text{m}$  for the respective sampling depths. Samples from sea surface microlayer (SML) as red-filled, underlying water (ULW) as blue-filled, Surface as red-striped, and ULW-Net as blue-striped boxes.



30

**Figure S 6:** Concentration differences during low pico- and nanophytoplankton abundance (Low P/NP) and high pico- and nanophytoplankton abundance (High P/NP) conditions for (a) total amino acids (TAA), (b) total combined carbohydrates (TCCHO), (c) surfactants (SA), (d) total organic carbon (TOC), (e) particulate organic carbon (POC) >20  $\mu\text{m}$ , (f) cyanobacteria biomass >20  $\mu\text{m}$ , (g) particulate amino acids (PAA) >20  $\mu\text{m}$  and (h) particulate combined carbohydrates (PCCHO) >20  $\mu\text{m}$  for the respective sampling depths. Samples from sea surface microlayer (SML) as red-filled, underlying water (ULW) as blue-filled, Surface as red-striped, and ULW-Net as blue-striped boxes.

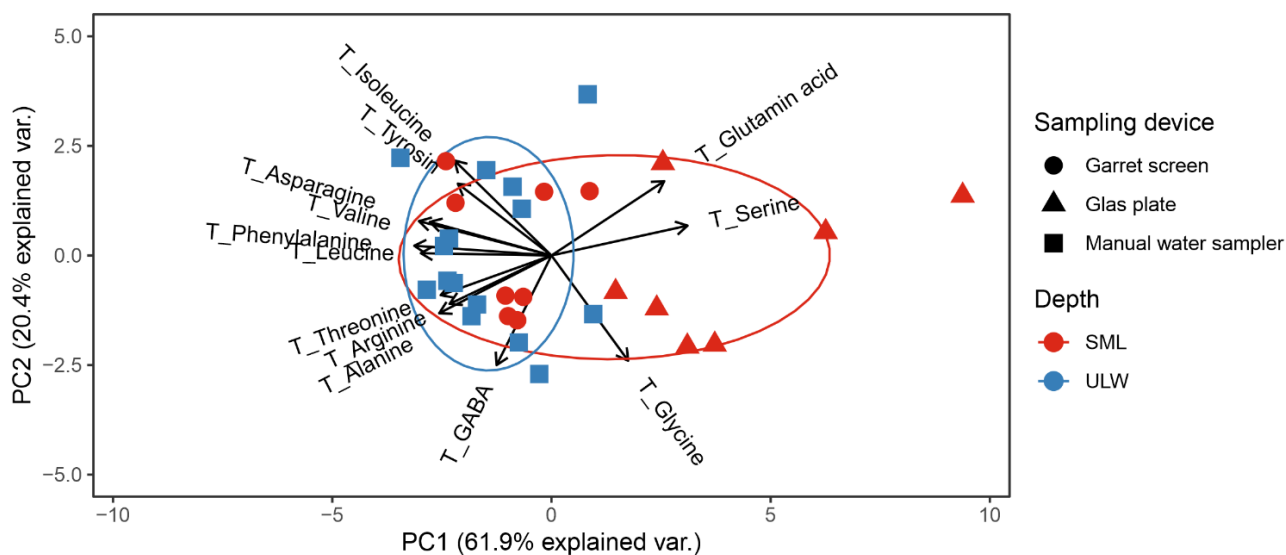
35



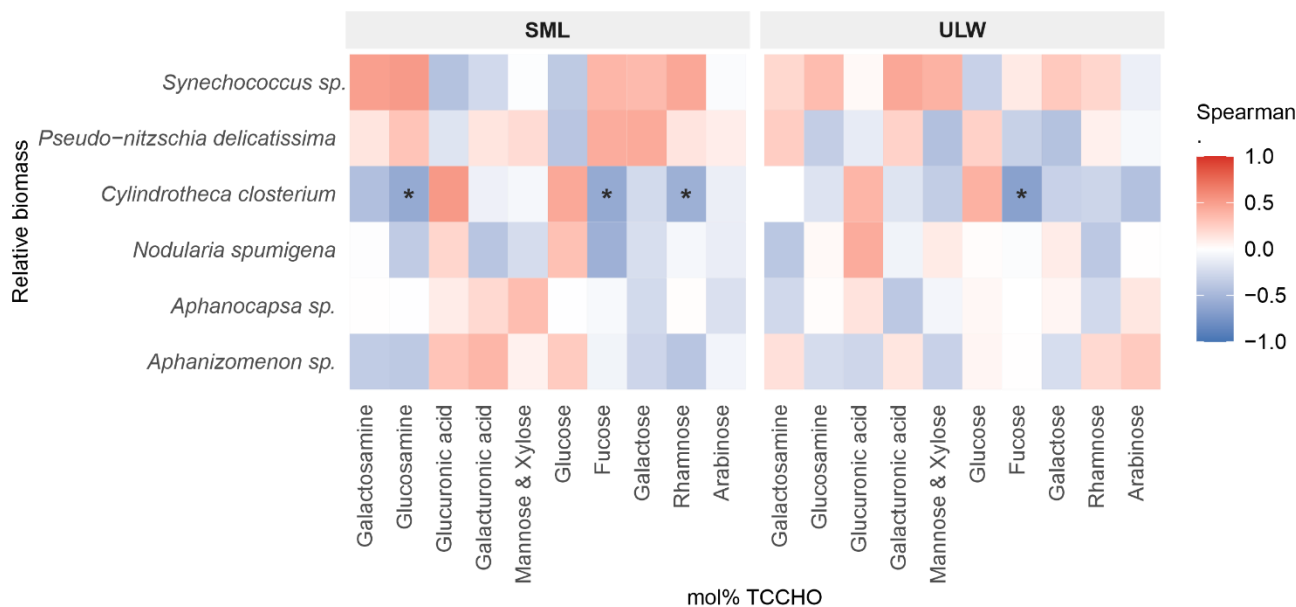
40

**Figure S 7:** Enrichment factors of (a) total organic carbon (TOC), (b) total combined carbohydrates (TCCHO), (c) total amino acids (TAA), and (d) surfactants across stations. Yellow circles indicate that the stations belong to the low pico- and nanophytoplankton abundance (Low P/NP) condition, and green circles indicate the high pico- and nanophytoplankton abundance (High P/NP) condition. The dashed horizontal line marks an enrichment factor of 1, representing equal concentrations in the SML and ULW.

45



50 **Figure S 8:** PCA biplots of total amino acids (TAA). Scores are colored by sea surface microlayer (SML, red) and underlying water (ULW, blue) and sampling devices are indicated with different shapes: Garrett screen in circles, glass plate in triangles and manually deployed water sampler in squares. Arrows show variable loadings; axes are scaled to unit variance and annotated with percent variance explained (PC1 61.9 %, PC2 20.4 %).



55

**Figure S 9:** Heatmaps of Spearman rank-order correlations ( $\rho$ ) between relative species-specific microphytoplankton and *Synechococcus sp.* biomass and total combined carbohydrates (TCCHO). Tile colors range from blue ( $\rho = -1$ ) through white ( $\rho = 0$ ) to red ( $\rho = +1$ ), and significant correlations are marked with asterisks (\*  $p < 0.05$ ; \*\*  $p < 0.01$ ; \*\*\*  $p < 0.001$ ).

### 3. Discussion

#### Comparison of glass plate and Garrett screen SML sampling

Seawater was sampled from the sea surface microlayer (SML) using a glass plate or a Garrett screen and from the underlying water (ULW) by a manually operated 2 L water sampler (Hydrobios, according to Ruttner). Glass plate sampling of the SML and sampling of the corresponding ULW was conducted from a working boat. When bad weather conditions prevented the deployment of the working boat, SML and ULW samples were instead collected from the bow of the vessel. In these cases, the SML was sampled using a Garrett screen. The amino acid composition obtained from the different sampling methods is presented in Fig. S8. While the compositions derived from Garrett screen and ULW samples largely overlap, those obtained using the glass plate show a separation from the others.

Meteorological conditions exert a strong control on the physical structure, composition, and persistence of the SML. Wind speed is a primary driver, influencing both SML thickness and organic matter enrichment. While earlier studies suggested disruption above  $\sim 5 \text{ m s}^{-1}$ , subsequent work has shown that surfactant enrichment can persist at wind speeds of up to  $10 \text{ m s}^{-1}$  (Wurl et al., 2011). Nevertheless, increasing wind enhances mixing with underlying water, reducing SML thickness and the enrichment of particulate organic matter (Liu and Dickhut, 1998), and alters biogenic particle structure, with gel-like particles accumulating under calm conditions but breaking down or being removed at higher wind speeds (Sun et al., 2018). Meteorological conditions also affect sampling outcomes. Under high wind conditions, methods such as glass plates and Garrett screens may collect thicker layers and include more subsurface water, potentially diluting the SML signal (Cunliffe & Murrell, 2009; Wong et al., 2021). Precipitation further modifies SML properties by introducing freshwater signals and transient stratification, particularly under low wind conditions, while higher winds promote rapid mixing (Gassen et al., 2024).

Sampling approaches such as glass plates and Garrett screens collect layers of substantially different thickness ( $\sim 30\text{--}60 \mu\text{m}$  vs.  $200\text{--}500 \mu\text{m}$ ) (Kuznetsova et al., 2004; Engel and Galgani, 2016), which can lead to dilution of surface-enriched compounds, e.g. amino acids and carbohydrates, with underlying water in thicker samples (Dreshchinskii and Engel, 2017). Glass plates preferentially collect hydrophobic amino acids and surface-active materials, while screens better recover phytoplankton organisms and particulate matter (Momzikoff et al., 2004). Overall, while qualitative compositional patterns between SML and ULW are generally robust, absolute differences, e.g., for dissolved fractions, should be interpreted with caution due to potential method-dependent dilution effects. This difference may partly reflect the meteorological conditions under which the respective sampling methods were applied, as Garrett screen sampling was primarily conducted during bad weather conditions (high wind speeds, wave action, and occasional rain), while glass plate sampling could only be performed under calmer conditions from the working boat.

Overall, the SML is a highly dynamic system, and both its properties and their measurement are strongly influenced by short-term meteorological forcing. As glass plate and Garrett screen sampling were not conducted in parallel in our study, it is not possible to disentangle methodological effects from environmental variability in the present dataset. However, all methods

applied here follow established community standards. Therefore, methodological differences alone are unlikely to fully account for the observed molecular contrasts between SML and ULW samples.

95

#### 4. References

- Cunliffe, M. and Murrell, J. C.: The sea-surface microlayer is a gelatinous biofilm, *ISME J*, 3, 1001–1003, <https://doi.org/10.1038/ismej.2009.69>, 2009.
- 100 Dreshchinskii, A. and Engel, A.: Seasonal variations of the sea surface microlayer at the Boknis Eck Times Series Station (Baltic Sea), *J Plankton Res*, 39, 943–961, <https://doi.org/10.1093/plankt/fbx055>, 2017.
- Engel, A. and Galgani, L.: The organic sea-surface microlayer in the upwelling region off the coast of Peru and potential implications for air-sea exchange processes, *Biogeosciences*, 13, 989–1007, <https://doi.org/10.5194/bg-13-989-2016>, 2016.
- 105 Gassen, L., Ayim, S. M., Badewien, T. H., Ribas-Ribas, M., & Wurl, O.: Wind speed effects on rainfall-induced salinity and temperature anomalies at the sea surface microlayer at mid-latitudes, *Elem Sci Anth*, 12, 00004, <https://doi.org/10.1525/elementa.2024.00004>, 2024.
- 110 Kuznetsova, M., Lee, C., Aller, J., & Frew, N.: Enrichment of amino acids in the sea surface microlayer at coastal and open ocean sites in the North Atlantic Ocean, *Limnol. Oceanogr.*, 49, 1605-1619, <https://doi.org/10.4319/lo.2004.49.5.1605>, 2004.
- Liu, K., & Dickhut, R. M.: Effects of wind speed and particulate matter source on surface microlayer characteristics and enrichment of organic matter in southern Chesapeake Bay, *J. Geophys. Res. Atmos.*, 103, 10571-10577, <https://doi.org/10.1029/97JD03736>, 1998.
- Momzikoff, A., Brinis, A., Dallot, S., Gondry, G., Saliot, A., & Lebaron, P.: Field study of the chemical characterization of the upper ocean surface using various samplers, *Limnol. Oceanogr. Methods*, 2, 374-386, <https://doi.org/10.4319/lom.2004.2.374>, 2004.
- 120 Van Pinxteren, M., Müller, C., Iinuma, Y., Stolle, C., and Herrmann, H.: Chemical characterization of dissolved organic compounds from coastal sea surface microlayers (Baltic Sea, Germany), *Environ Sci Technol*, 46, 10455–10462, <https://doi.org/10.1021/es204492b>, 2012.
- 125 Reinthaler, T., Sintes, E., & Herndl, G. J.: Dissolved organic matter and bacterial production and respiration in the sea-surface microlayer of the open Atlantic and the western Mediterranean Sea, *Limnol. Oceanogr.*, 53, 122-136, <https://doi.org/10.4319/lo.2008.53.1.0122>, 2008.
- 130 Sun, C. C., Sperling, M., & Engel, A.: Effect of wind speed on the size distribution of gel particles in the sea surface microlayer: insights from a wind–wave channel experiment. *Biogeosciences*, 15, 3577-3589, <https://doi.org/10.5194/bg-15-3577-2018>, 2018.
- 135 Wong, S. K., Suzuki, S., Cui, Y., Kaneko, R., Kogure, K., & Hamasaki, K.: Sampling constraints and variability in the analysis of bacterial community structures in the sea surface microlayer, *Front. Mar. Sci.*, 8, 696389, <https://doi.org/10.3389/fmars.2021.696389>, 2021.
- Wurl, O., Wurl, E., Miller, L., Johnson, K., and Vagle, S.: Formation and global distribution of sea-surface microlayers, *Biogeosciences*, 8, 121–135, <https://doi.org/10.5194/bg-8-121-2011>, 2011.